Yan *et al. Nanoscale Research Letters* (2017) 12:553
DOI 10.1186/s11671-017-2321-4

Nanoscale Research Letters

NANO EXPRESS Open Access

Temperature Dependence of Spin-Split Peaks in Transverse Electron Focusing

Chengyu Yan[1,2*], Sanjeev Kumar[1,2], Michael Pepper[1,2], Patrick See[3], Ian Farrer[4], David Ritchie[4], Jonathan Griffiths[4] and Geraint Jones[4]

Abstract

We present experimental results of transverse electron-focusing measurements performed using n-type GaAs. In the presence of a small transverse magnetic field ($B_\perp$), electrons are focused from the injector to detector leading to focusing peaks periodic in $B_\perp$. We show that the odd-focusing peaks exhibit a split, where each sub-peak represents a population of a particular spin branch emanating from the injector. The temperature dependence reveals that the peak splitting is well defined at low temperature whereas it smears out at high temperature indicating the exchange-driven spin polarisation in the injector is dominant at low temperatures.

Keywords: Spintronics, Ballistic transport, Transverse electron focusing

Background

The electron transport through a quasi one-dimensional (1D) system realised using the two-dimensional electron gas (2DEG) formed at the interface of GaAs/AlGaAs heterostructure has been extensively studied. A 1D system provides an outstanding platform to envisage not only the non-interacting quantum mechanical system where the conductance quantisation [1–3] is in the units of $n \times \frac{2e^2}{h}$, where $n = 1, 2, 3...$ are different 1D energy subbsands, but also a venue to explore many-body physics [4–9]. Recently, the progress in the physics of many-body 1D system has gained momentum due to prediction and experimental demonstration of rich phases in low-density 1D system leading to incipient Wigner crystallisation [6, 7, 10]. Moreover, the origin of the 0.7 conductance anomaly in the framework of many-body 1D system is still debated [11–15]. The 0.7 anomaly has two major features: first, in the presence of an in-plane magnetic field, the 0.7 anomaly evolves into $0.5 \times \frac{2e^2}{h}$ plateau, which indicates it is spin-related [4]; second, the 0.7 anomaly was found to weaken (strengthen) with decreasing (increasing) temperature [4]. These remarkable observations have led to a volume of theoretical and experimental attempts to probe the intrinsic spin polarisation associated with the 0.7 anomaly; however, there is no consensus as such on the origin of this anomaly [11–15]. Therefore, to shed more light on the 0.7 anomaly, it is essential to perform a direct measurement on the spin polarisation within a 1D channel.

A scheme based on transverse electron focusing (TEF) was proposed to address the spin polarisation [16, 17] and was validated in p-type GaAs [18, 19] and n-type InSb [20]. Within this scheme, the spin polarisation arising from the exchange interaction can be extracted from the asymmetry of the two sub-peaks of the first focusing peak. Recently, we showed that injection of 1D electrons whose spins have been spatially separated can be detected in the form of a split in the first focusing peak, where the two sub-peaks represent the population of detected spin states [21]. In the present work, we report the temperature dependence of spin-split first focusing peak and analyse the results based on the spin-gap present between the two spin species.

Method

The devices studied in the present work were fabricated from the high mobility two-dimensional electron gas (2DEG) formed at the interface of $GaAs/Al_{0.33}Ga_{0.67}As$ heterostructure. At 1.5 K, the measured electron density (mobility) was $1.80 \times 10^{11} cm^{-2} (2.17 \times 10^6 cm^2 V^{-1} s^{-1})$

*Correspondence: uceeya3@ucl.ac.uk
[1] London Centre for Nanotechnology, 17-19 Gordon Street, London WC1H 0AH, United Kingdom
[2] Department of Electronic and Electrical Engineering, University College London, Torrington Place, London WC1E 7JE, United Kingdom
Full list of author information is available at the end of the article

therefore, the mean free path is over 10 μm which is much larger than the electron propagation length. The experiments were performed in a cryofree dilution refrigerator with a lattice temperature of 20 mK using the standard lock-in technique. The range of temperature dependence measurement was from 20 mK to 1.8 K.

Results and discussion

Figure 1a shows the experimental setup along with a typical focusing spectrum obtained using the device shown in the inset. The focusing device is specially designed so that the injector and detector can be controlled separately to avoid a possible cross-talking between them [21–23]. The quantum wire used for the injector and detector has a width (confinement direction) of 500 nm and length (current flow direction) of 800 nm. Both the injector and detector show well-defined conductance plateaus as shown in Fig. 1b. Further details on the device are given in the caption of Fig. 1.

With negative magnetic field, the measured signal is almost zero because electrons bend into the opposite direction and thus miss the detector. It is also evident that the Shubnikov-de Haas oscillation and quantum Hall effect do not contribute to the observation. In the presence of a small positive transverse magnetic field ($B_\perp$) electrons are focused from the injector to detector leading to focusing peaks periodic in $B_\perp$ while the detected signal is negligible at the negative magnetic field end. The calculated periodicity of 60 mT using the relation [23],

$$B_{focus} = \frac{\sqrt{2}\hbar k_F}{eL} \tag{1}$$

is in good agreement with the experimental result. Here, e is the elementary charge and $\hbar$ is the reduced Planck constant, L is the separation between the injector and detector (in the 90° focusing device geometry, this is the separation along the diagonal direction). In addition to the periodic focussing peak which is a manifestation of the semi-classical electron cyclotron orbit, it is interesting to notice the splitting of odd-numbered focusing peaks. It is suggested that this anomalous splitting of odd-numbered focusing peaks arises from the spin-orbit interaction (SOI) [16, 17] and has been successfully observed in GaAs hole gas [18, 19] and InSb electron gas [20]. We recently demonstrated splitting of odd-numbered focusing peaks in n-GaAs [21] where a longer quantum wire possessing partially polarised and spatially separated 1D electrons was used to inject the polarised 1D electrons into the 2D regime and subsequently measured across the detector in the form of a split in the first focusing peak. Here, we are interested in investigating the thermal effect on the spin states within the 1D channel via the transverse electron focusing. We note that the splitting smears out when the thermal energy k_BT exceeds $2\Delta E$ (ΔE is the energy difference between the two spin branches) agreeing with the theoretical prediction [17].

Before we discuss the temperature dependence effect, it is important to understand the mechanism responsible for the observed peak splitting. Figure 2a, b shows the potential profile of the split gates forming the injector (bottom pair) and the detector (left pair). In the presence of SOI, the two spin species follow different cyclotron radii as shown in Fig. 2a thus resulting in two sub-peaks in the first focusing peak. However, the situation is different for the second focusing peak where a scattering at the boundary of electrostatic potential created by the split gates is involved as shown in Fig. 2b. In this case, a spin-up electron (red arrow in the colourplots) initially

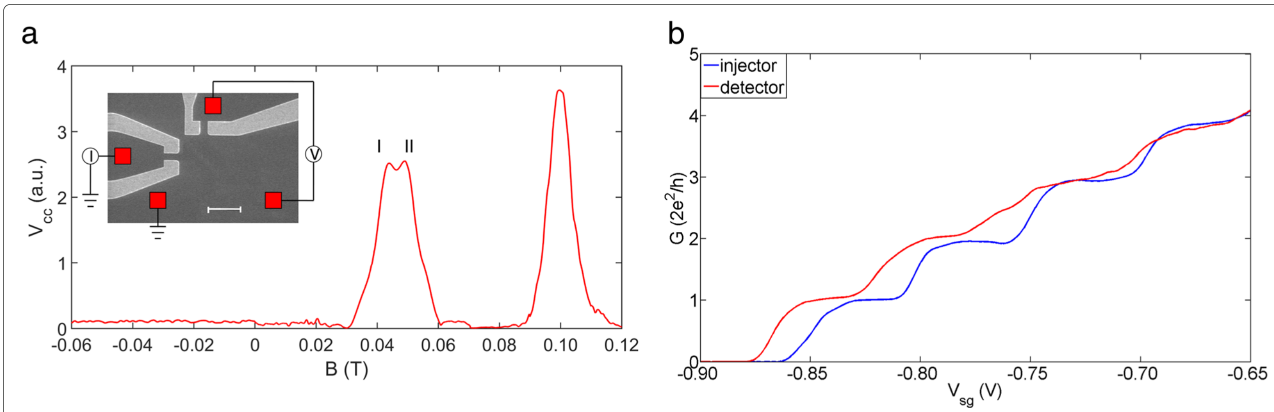

Fig. 1 The experiment setup and device characteristic. **a** A representative plot of transverse electron focusing with both the injector and detector set to G_0 ($2e^2/h$). V_{cc} is the voltage drop across the detector. Focusing peaks are well defined with a positive magnetic field, and the signal is negligible with a negative magnetic field. The first peak shows pronounced splitting. The two sub-peaks have been highlighted as peak I and peak II. The inset shows an SEM image of the device. The separation between the injector and detector is 1.5 μm. Red squares form the Ohmic contacts whereas two pairs of grey-coloured gates, left and top, form the injector and detector, respectively. The scale bar is 2 μm. **b** Conductance characteristics of the injector and detector

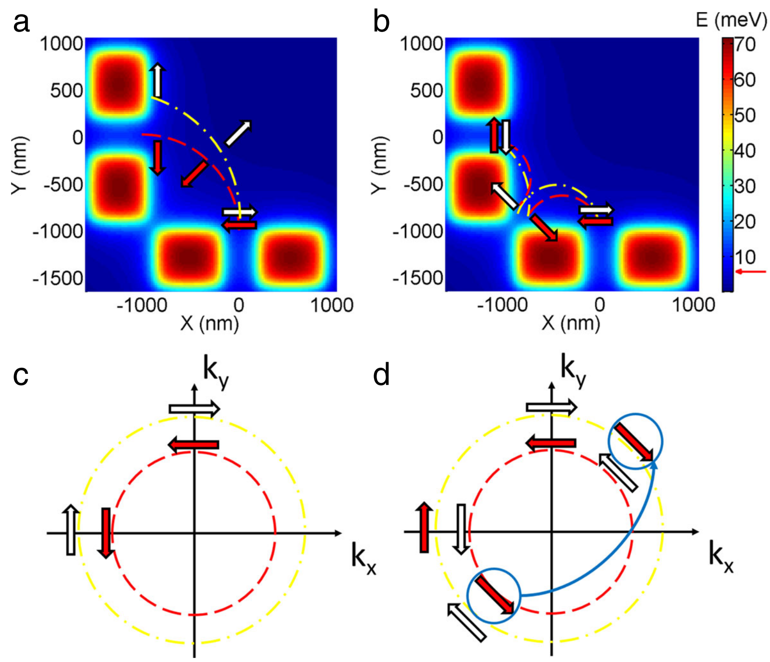

Fig. 2 Mechanism of peak splitting. **a**, **b** Peak splitting in the coordinate space for first and second focusing peaks, respectively. The red and white arrows represent spin-up and spin-down electrons, the coloured blocks stand for the electrostatic potential and the red-dashed trace is with smaller cyclotron radius while the yellow-dotted one is with larger cyclotron radius. **c**, **d** Peak splitting in the k-space for the first and second focusing peaks, respectively. The electrons travel from (0, k_y) to (-k_x, 0) anticlockwise in plot (**c**). In plot (**d**), the thick blue arrow highlights the transition after reflection at the boundary of electrostatic potential formed between the injector and detector

follows a smaller cyclotron radius while it possesses a larger radius after the scattering [16, 17] and vice-versa for the spin-down electron (white arrow), thus the two spin species re-join at the detector. The underneath reasoning for the peak splitting can be found in the k-space in Fig. 2c, d. Here, we assume the spin-orbit interaction is of Rashba-type; however, the analysis holds valid for Dresselhaus effect in bulk as well. For the first focusing peak (Fig. 2c), the two spin-species travel from (0, k_y) to (-k_x, 0) along different Fermi surfaces. For the second focusing peak (Fig. 2d), the same argument holds true before the scattering; however, the momentum changes its sign while the spin orientation remains preserved after the scattering [16]. Therefore, a spin-up electron (red arrows) initially occupying the inner Fermi surface hops to the outer Fermi surface after the scattering to guarantee that both the sign of the momentum and the spin orientation are in the correct order (the hopping is highlighted by the thick blue arrow in Fig. 2d) and vice-versa for the spin-down electron. The cyclotron radius is proportional to the momentum, so that the alternation in cyclotron radius occurs in the coordinate space as a consequence of hopping between two Fermi surfaces which leads to a single second focusing peak.

Figure 3a–c shows the temperature dependence of focusing results with injector set to $0.5G_0$, G_0 and $1.8G_0$, respectively, where the lattice temperature is incremented from 20 mK (the electron temperature is calibrated to be around 70 mK) to 1.8 K, and Fig. 3d–f shows the zoom-in of the data in Fig. 3a–c, respectively. For $G_i = 0.5G_0$ (Fig. 3a) a single peak is observed (as only one spin-subband is occupied), which broadens gradually at higher temperature. In addition, the focusing peak shifts towards the center of the spectrum and becomes more symmetric at higher temperature (see the bottom trace, $T = 1.8$ K, Fig. 3a, d). This may be due to a possible electron transition between the two spin-subbands at relatively high temperature. In comparison, for $G_i = G_0$ (Fig. 3b), the sub-peaks, each representing a spin-state, are present from 20 mK up to 1.2 K. However, the dip in the first focusing peak leading to two sub-peaks smears out at 1.8 K (Fig. 3b, e). With G_i set to 1.8 G_0 (Fig. 3c), the splitting is not well resolved and the left sub-peak (I) dominates the spectrum. We note that on increasing the temperature, the peak I gradually reduced in amplitude to result in an asymmetric first focusing peak at 1.8 K. In n-type InSb, the splitting was pronounced even at 10 K, which is consistent with the fact the peak splitting was around 60 mT, an indication of strong SOI in InSb [20], which is one order larger than the peak splitting of 5.5 mT measured in the present case.

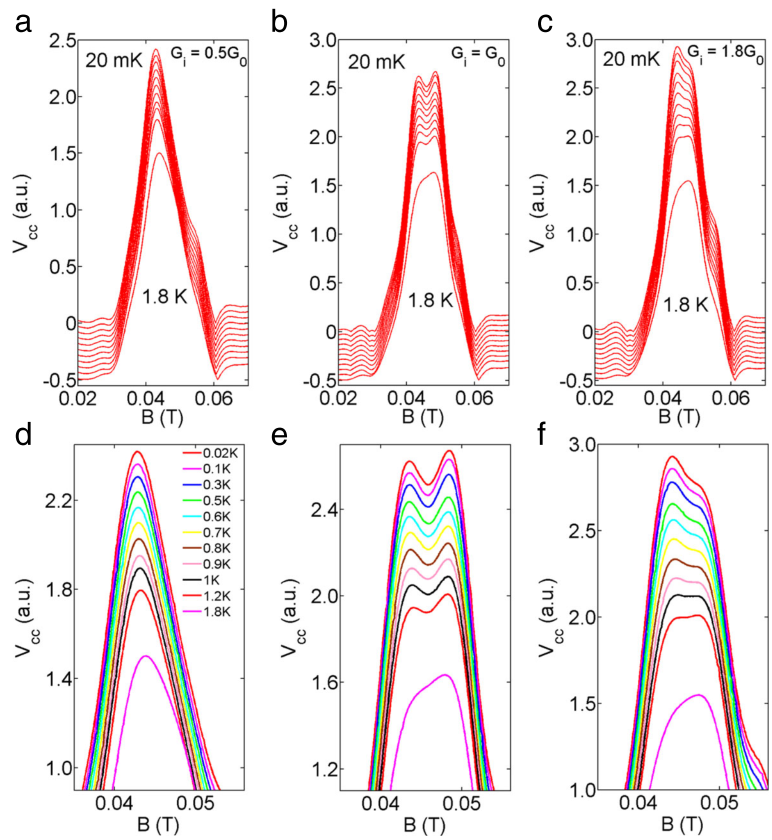

Fig. 3 Temperature dependence of TEF. **a**–**c** The injector was set to $0.5G_0$, G_0 and $1.8G_0$, respectively. The lattice temperature was incremented from 20 mK (top trace) to 1.8 K (bottom trace). Data have been offset vertically for clarity. **d**-**f**, zoom-in of the data in (**a**)-(**c**)

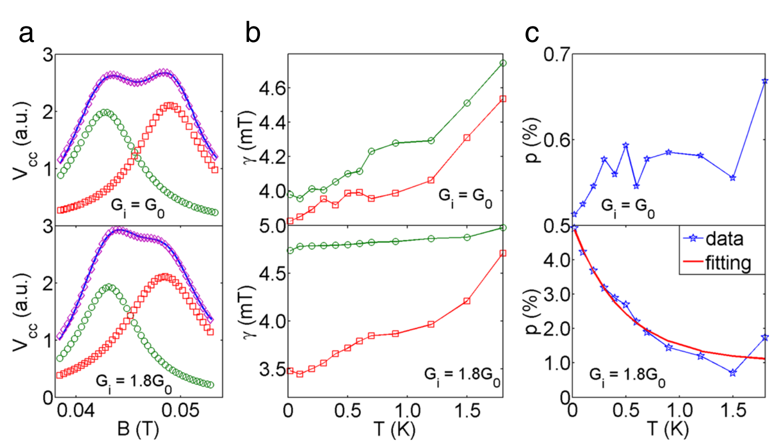

Fig. 4 Analysis of the temperature dependence data. The plots on the top are for $G_i = G_0$, the bottom ones are for $G_i = 1.8\, G_0$. **a** Reconstructing the first focusing peak with two Lorentzian peaks at 20 mK. The solid blue line is the experimental data, the green round marker is the fit for peak I, the red square marker is the fit for peak II and the magenta diamond marker highlights the reconstructed focusing peak. **b** FHWM, γ as a function of temperature: the sub-peaks broaden with increasing temperature in both cases. The markers represent the same meaning as in plot (**a**). **c** The polarisation measured with $G_i = G_0$ fluctuates around 0.6%. On the other hand, the polarisation measured with $G_i = 1.8\, G_0$ follows an exponential decay

To extract the peak width and amplitude accurately considering the two sub-peaks may partially overlap with each other, we use two Lorentzian peaks to reconstruct the experimental data as shown in Fig. 4a using the relation,

$$A(B) = \sum_{i=1,2} A_i \times \frac{\gamma_i^2}{\gamma_i^2 + (B - B_i)^2} \quad (2)$$

where A_i is the amplitude of the peak i (i =1, 2 for peak I and peak II, respectively), γ_i denotes the full width at half maximum (FWHM), and B_i is the center of the peak. Two noticeable results can be extracted from the fitting: first, it is seen from Fig. 4b that γ (see caption of Fig. 4 for details on traces and symbols representing peak I and peak II) for both peak I and peak II increases with rising temperature regardless of the injector conductance which indicates the thermal broadening of the sub-peaks prevents the observation of peak splitting at high temperature. It may be noted that peak I for G_i = $1.8G_0$ is relatively robust against temperature compared to other peaks (both peaks of G_0 and peak II of $1.8G_0$). Second, the measured spin polarization p $\left(p = \left|\frac{A_1 - A_2}{A1 + A_2}\right|\right)$ with G_i = G_0 fluctuates around 0.6% and shows no explicit temperature dependence which agrees with the fact that spin polarisation at conductance plateau should remain at 0 regardless of the temperature (Fig. 4c, upper plot). On the other hand, when G_i is set to 1.8 G_0, the extracted spin polarisation decays from 5 to 0.8% (Fig. 4d, lower plot) following the relation [15],

$$p = \alpha exp\left(-\frac{k_B T}{\Delta E}\right) + c \quad (3)$$

where α is a prefactor accounting for the amplitude, k_B is the Boltzmann constant, ΔE is the energy difference between the two spin-branches and c accounts for the small residual value that arises from the uncertainty in the experiment. We extracted the value of ΔE to be around 0.041 meV (corresponding to 0.5 K). The theory [17] predicts the splitting should persist until $k_B T$ exceeds $2\Delta E$ (i.e. 1 K in our case) which agrees reasonably well with our result that the peak splitting is observable up to 1.2 K.

Conclusion

In conclusion, we showed the temperature dependence of the transverse electron focusing where the contribution of the two spin states manifested as two sub-peaks in the first focusing peak. It was observed that the peak splitting is well defined from 20 mK up to 1.2 K and beyond this temperature the peak splitting smeared out. Moreover, the focusing peak has a tendency to become more symmetric at higher temperature indicating a possible equilibrium between the two spin branches due to thermal excitation.

The work is funded by the Engineering and Physical Sciences Research Council (EPSRC), UK.

Authors' contributions

CY in consultation with SK conceived and designed the experiments; CY and SK performed the measurement; CY, SK and MP analysed the data; PS fabricated the devices; JG and GJ did e-beam lithography; IF and DR grew the wafer; CY and SK wrote the paper with inputs from MP, and other co-authors. All authors read and approved the final manuscript.

Competing interests

The authors declare that they have no competing interests.

Publisher's Note

Received: 4 August 2017 Accepted: 16 September 2017
Published online: 26 September 2017

References

1. Thornton TJ, Pepper M, Ahmed H, Andrews D, Davies GJ (1986) One-dimensional conduction in the 2D electron gas of a GaAs-AlGaAs heterojunction. Phys Rev Lett 56:1198–1201. doi:10.1103/PhysRevLett.56.1198
2. Wharam DA, Thornton TJ, Newbury R, Pepper M, Ahmed H, Frost JEF, Hasko DG, Peacock DC, Ritchie DA, Jones GAC (1988) One-dimensional transport and the quantisation of the ballistic resistance. J Phys C Solid State Phys 21(8):209
3. van Wees BJ, van Houten H, Beenakker CWJ, Williamson JG, Kouwenhoven LP, van der Marel D, Foxon CT (1988) Quantized conductance of point contacts in a two-dimensional electron gas. Phys Rev Lett 60:848–850. doi:10.1103/PhysRevLett.60.848
4. Thomas KJ, Nicholls JT, Simmons MY, Pepper M, Mace DR, Ritchie DA (1996) Possible spin polarization in a one-dimensional electron gas. Phys Rev Lett 77:135–138. doi:10.1103/PhysRevLett.77.135
5. Sfigakis F, Ford CJB, Pepper M, Kataoka M, Ritchie DA, Simmons MY (2008) Kondo effect from a tunable bound state within a quantum wire. Phys Rev Lett 100:026807. doi:10.1103/PhysRevLett.100.026807
6. Hew WK, Thomas KJ, Pepper M, Farrer I, Anderson D, Jones GAC, Ritchie DA (2009) Incipient formation of an electron lattice in a weakly confined quantum wire. Phys Rev Lett 102:056804. doi:10.1103/PhysRevLett.102.056804
7. Kumar S, Thomas KJ, Smith LW, Pepper M, Creeth GL, Farrer I, Ritchie D, Jones G, Griffiths J (2014) Many-body effects in a quasi-one-dimensional electron gas. Phys Rev B 90:201304. doi:10.1103/PhysRevB.90.201304
8. Yan C, Kumar S, Pepper M, See P, Farrer I, Ritchie D, Griffiths J, Jones G (2017) Fano resonance in a cavity-reflector hybrid system. Phys Rev B 95:041407. doi:10.1103/PhysRevB.95.041407
9. Yan C, Kumar S, Pepper M, See P, Farrer I, Ritchie D, Griffiths J, Jones G (2017) Interference effects in a tunable quantum point contact integrated with an electronic cavity. Phys Rev Appl 8:024009. doi:10.1103/PhysRev-Applied.8.024009
10. Meyer JS, Matveev KA (2009) Wigner crystal physics in quantum wires. J Phys Condens Matter 21(2):023203
11. Wang CK, Berggren KF (1996) Spin splitting of subbands in quasi-one-dimensional electron quantum channels. Phys Rev B 54:14257–14260. doi:10.1103/PhysRevB.54.R14257
12. Wang CK, Berggren KF (1998) Local spin polarization in ballistic quantum point contacts. Phys Rev B 57:4552–56. doi:10.1103/PhysRevB.57.4552
13. Reilly DJ, Buehler TM, O'Brien JL, Hamilton AR, Dzurak AS, Clark RG, Kane BE, Pfeiffer LN, West KW (2002) Density-dependent spin polarization in ultra-low-disorder quantum wires. Phys Rev Lett 89:246801. doi:10.1103/PhysRevLett.89.246801
14. Reilly DJ (2005) Phenomenological model for the 0.7 conductance feature in quantum wires. Phys Rev B 72:033309. doi:10.1103/PhysRevB.72.033309
15. Bruus H, Cheianov VV, Flensberg K (2001) The anomalous 0.5 and 0.7 conductance plateaus in quantum point contacts. Physica E: Low-dimensional Syst Nanostruct 10(1):97–102. doi:10.1016/S1386-9477(01)00061-3
16. Usaj G, Balseiro CA (2004) Transverse electron focusing in systems with spin-orbit coupling. Phys Rev B 70:041301. doi:10.1103/PhysRevB.70.041301

17. Reynoso A, Usaj G, Balseiro CA (2007) Detection of spin polarized currents in quantum point contacts via transverse electron focusing. Phys Rev B 75:085321. doi:10.1103/PhysRevB.75.085321
18. Rokhinson LP, Pfeiffer LN, West KW (2006) Spontaneous spin polarization in quantum point contacts. Phys Rev Lett 96:156602. doi:10.1103/PhysRevLett.96.156602
19. Chesi S, Giuliani GF, Rokhinson LP, Pfeiffer LN, West KW (2011) Anomalous spin-resolved point-contact transmission of holes due to cubic Rashba spin-orbit coupling. Phys Rev Lett 106:236601. doi:10.1103/PhysRevLett.106.236601
20. Dedigama AR, Deen D, Murphy SQ, Goel N, Keay JC, Santos MB, Suzuki K, Miyashita S, Hirayama Y (2006) Current focusing in InSb heterostructures. Physica E: Low-dimensional Syst Nanostruct 34(1):647–50. doi:10.1016/j.physe.2006.03.050
21. Yan C, Kumar S, Thomas K, Pepper M, See P, Farrer I, Ritchie D, Griffiths JP, Jones GAC (2017) Direct observation of exchange-driven spin interactions in one-dimensional system. Appl Phys Lett 111(4):042107. doi:10.1063/1.4989374
22. Potok RM, Folk JA, Marcus CM, Umansky V (2002) Detecting spin-polarized currents in ballistic nanostructures. Phys Rev Lett 89:266602. doi:10.1103/PhysRevLett.89.266602
23. van Houten H, Beenakker CWJ, Williamson JG, Broekaart MEI, van Loosdrecht PHM, van Wees BJ, Mooij JE, Foxon CT, Harris JJ (1989) Coherent electron focusing with quantum point contacts in a two-dimensional electron gas. Phys Rev B 39:8556–75. doi:10.1103/PhysRevB.39.8556